

An Adaptive Placement and Parallelism Framework for Accelerating RLHF Training

Youshao Xiao, Weichang Wu, Zhenglei Zhou, Fagui Mao, Shangchun Zhao,

Lin Ju, Lei Liang, Xiaolu Zhang, Jun Zhou,

Ant Group, Hangzhou, Zhejiang

{youshao.xys,jiuyue.wwc,zhouzhenglei.zzl,maofagui.mfg,shangchun.zsc,julin.jl,leywar.liang}@antgroup.com

{yueyin.zxl,jun.zhoujun}@antfin.com

arXiv:2312.11819v2 [cs.LG] 25 Jan 2024

Abstract—Recently, ChatGPT or InstructGPT like large language models (LLM) has made a significant impact in the AI world. Many works have attempted to reproduce the complex InstructGPT’s training pipeline, namely Reinforcement Learning with Human Feedback (RLHF). However, the mainstream distributed RLHF training methods typically adopt a fixed model placement strategy, referred to as the Flattening strategy. This strategy treats all four interdependent models involved in RLHF as a single entity, distributing them across all devices and applying parallelism techniques designed for a single model, regardless of the different workloads inherent to each model. As a result, this strategy exacerbates the generation bottlenecks in the RLHF training and degrades the overall training efficiency. To address these issues, we propose an adaptive model placement framework that offers two flexible model placement strategies. The Interleaving strategy helps reduce memory redundancy and communication costs of RLHF training by placing models without dependencies on exclusive devices with careful orchestration. On the other hand, the Separation strategy improves the throughput of model training by separating the training and inference runtime of the RLHF pipeline with additional shadow models. Furthermore, our framework provides a simple user interface and allows for the agile allocation of models across devices in a fine-grained manner for various training scenarios, involving models of varying sizes and devices of different scales. Extensive experiments have demonstrated that our Interleaving and Separation strategies can achieve notable improvements up to $11\times$, compared to the current state-of-the-art (SOTA) approaches. The results highlight the effectiveness and adaptability of our approaches in accelerating the training of distributed RLHF.

Index Terms—Distributed Training, Large Language Model, RLHF, Heterogeneous Hardware

I. INTRODUCTION

Large Language Models (LLMs) have demonstrated remarkable capabilities across various natural language processing tasks [2], [5], [29], [35]. However, it is crucial to fine-tune LLM models to align them with human preferences. In the absence of proper alignment with human feedback, LLMs may exhibit behaviors that deviate from expectations. These behaviors include generating fabricated information, pursuing inaccurate objectives, and producing harmful, misleading, and biased expressions [8], [13], [18]). To tackle this issue, researchers have proposed a series of approaches aimed at ensuring that LLMs adhere to ethical considerations and societal norms.

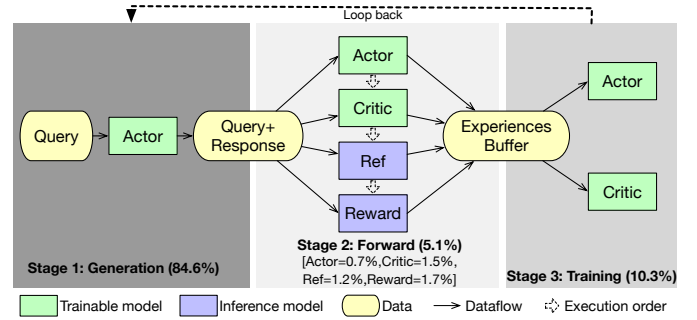


Fig. 1. Workflow of RLHF and Percentage (in %) of Each Stage Duration.

One of the most successful approaches in addressing the alignment issue is Reinforcement Learning from Human Feedback [1], [18], [25]. Particularly, the pipeline proposed in InstructGPT [18], a sibling model of ChatGPT, has gained significant attention. RLHF combines human alignment with Reinforcement Learning (RL), a decision-making approach that allows AI agents to learn from interactions with the environment, receiving feedback in the form of rewards. This integration of RL with Human Feedback (HF) enables researchers to enhance the capabilities of LLMs and improve their alignment with human values. RLHF represents a significant advancement in building more reliable and responsible LLMs.

The predominant RL algorithm to finetune LLM is Proximal Policy Optimization (PPO) [21]. It is the main process in the RLHF pipeline known as “Step-3: Training RL Policy” in InstructGPT. This process leverages an Actor-Critic architecture [16], comprising four **interconnected** models: a Reference (Ref) model, a Reward model, an Actor model, and a Critic model. The pipeline is segmented into three sequential stages—generation, forward, and training—as depicted in Figure 1. Note that Actor and Critic models are **trainable models**, which are leveraged for *both training and inference runtime* while Ref and Reward models are **inference models** utilized *solely for inference*. Specifically, in the generation stage, the Actor model generates the response from the query. In the subsequent forward stage, given the query and response, all four models follow a **sequential execution order** to produce intermediate output results such as logits or values. For example, the Actor, Reference, Reward, and Critic components conduct

the forward stage one after the other. These results are stored in the experience replay buffer similar to DQN [17]. During the training stage, the Actor and Critic models are trained using batch data sampled from the buffer. This whole procedure repeats over a number of steps until converges. It is important to note that the Actor and Critic models utilize the same underlying model but under a **mixed usage of training and inference runtime** (inference are used in both generation or forward stage) across these three stages.

Across the training of RLHF, the size of individual LM parameters can exhibit significant variations, e.g. spanning from 7 billion (7B) to 65 billion (65B) parameters in models like the Llama series [26]. The presence of LMs in RLHF pipeline amplifies memory usage quadratically, which underscores the critical need for efficient distributed training methodologies. However, traditional distributed training techniques, such as data parallelism or model parallelism [10], [20], [24], [32], are primarily designed for training a single model, not for efficiently managing multiple interdependent models as seen in RLHF. This necessitates the development of innovative model placement strategies.

Existing works [3], [27], [33] typically employ a straightforward model placement strategy, namely **Flattening strategy**. *This strategy treats all involved models as a single entity and applies standard parallelism techniques designed for individual models.* While this strategy aligns well with the sequential execution order as the standalone PPO algorithm, it brings several limitations and opportunities for optimization. 1) This approach results in reduced memory available for a single model on each device. Therefore, we have to add up more devices and parallelism techniques to accommodate all four models, with increased memory redundancy and communication costs [20], [31]. 2) Different scales of model sizes require fine-grained model placement strategies. For instance, 7 billion-level models could be held by fewer devices compared with 65 billion-level models, which creates the opportunity for optimization. 3) The workloads during training and inference runtime inherently differ, necessitating distinct optimization techniques, such as distributed strategies. Specifically, in the training stage, it is advisable to shard the optimizer state, gradients, and parameters sequentially for better efficiency. On the other hand, during the inference stage, only the parameters need to be shared, as they are the only components utilized during inference.

Therefore, we propose the **Adaptive Placement and Parallelism (APP)** framework, which could significantly enhance the training efficiency in distributed RLHF training while ensuring no compromise on model performance. Firstly, our framework introduces two innovative model placement strategies to improve training efficiency in various RLHF training scenarios. Secondly, we design an APP Execution Engine abstraction that provides a user-friendly interface to modeling experts, shielding them from the intricate details of model placement and parallelism strategies.

Our work makes four main contributions:

i) **Adaptive Model Placement:** Our APP framework introduces two flexible model placement strategies. Our Interleaving

strategy places models without dependencies on exclusive devices and our Separation strategy decouples the training and inference runtime of the RLHF pipeline, significantly improving the training efficiency.

ii) **GPU Heterogeneity Support:** The Separation strategy accounts for mixed GPU capabilities, facilitating RLHF model training on a wider array of affordable and specialized GPU series for training or inference.

iii) **Enhanced Performance:** Our extensive experiments confirm that our method outperforms the state-of-the-art up to $11\times$ in terms of throughput.

iv) **Ease of Use:** The APP framework features an Execution Engine supporting various model placement strategies and acceleration techniques with minimal or no code changes. It makes the distributed RLHF training more accessible for users without expertise in distributed training.

Furthermore, we are actively working towards releasing the code for the APP framework as an open-source project.

II. BACKGROUND

A. Data and Model parallelism

According to different parallel objects, distributed training technology for parallelizing single language model can be divided into data parallelism and model parallelism.

Data Parallelism (DP) involves dividing the input data into multiple shards and assigning them to different devices for parallel processing. In traditional DP training methods like AllReduce [7], [22] or Distributed Data Parallel (DDP) [14], [19], each device holds a complete replica of the model states and uses the AllReduce primitive to synchronize the model states across devices. ZeRO (Zero Redundancy Optimizer) [20] is a technique that addresses memory redundancy of the model state replicas held on each device, which dominates the current LLM training. It categorizes the model states into three parts: optimizer states, gradients, and parameters. To optimize memory redundancy, ZeRO performs sequential optimization in three stages: ZeRO-1, ZeRO-2, and ZeRO-3. In ZeRO-1, only the optimizer states are sharded across devices, which requires communication in the parameter update stage. In ZeRO-2, the gradients are additionally sharded, introducing additional reduce-scatter communication after each backward stage. ZeRO-3 extendedly shards the model parameters to all devices, while it requires extra AllGather communication in both forward and backward stages. The increased level of ZeRO parallelism helps reduce memory redundancy but comes with increased communication costs [20], [31].

Model Parallelism, including Tensor and Pipeline Parallelism, involves distributing model parameters across multiple devices within or across instances [24]. Tensor Parallelism (TP) [23], [24] achieves this by vertically splitting the model, sharding tensors across multiple devices, and computing through distributed matrix multiplication. However, due to the frequent global communication, Tensor Parallelism is more efficient within a single node with a high GPU interconnect bandwidth. As the number of nodes increases, its scalability becomes limited. On the other hand, Pipeline Parallelism (PP) [9], [10]

adopts a horizontal model splitting approach, assigning different layers to different devices. It usually uses micro-batching to hide the bubbles which is the idle duration of the device in the pipeline.

B. Heterogeneous Network

Clusters with heterogeneous networks are common in the majority of cloud computing environments [12], where the bandwidth between intra-node and inter-node is unbalanced. For instance, in cloud A100 GPU clusters, NVLink/NVSwitch with a bandwidth up to 4.8Tbps is configured within the node. However, the inter-node bandwidth, which might utilize whether InfiniBand or Ethernet, typically ranges from 200Gbps to 800Gbps. Such disparities mean that the inter-node bandwidth can be approximately 24 times slower than the intra-node bandwidth [28], [31], [36]. This limitation becomes even more pronounced in heterogeneous GPU clusters, such as a mixture of A100 and V100, where different types of GPU devices can only be connected using Ethernet. The significant gap in bandwidth within and between nodes greatly hampers the communication efficiency of Tensor Parallelism and ZeRO, especially at higher levels of ZeRO [20], [31]. ZeRO-3, for instance, requires frequent AllGather communication primitives across all nodes to collect model parameters which are shared across all devices, as compared to ZeRO-2. Meanwhile, tensor parallelism requires more global communications for each matrix computation during computation. As a result, the inter-intra-node bandwidth gap will significantly hamper the efficiency of parallelism techniques. Moreover, as the size of the cluster scales out, the communication overhead caused by heterogeneous networks grows larger.

III. RELATED WORKS

Since the emergence of ChatGPT and InstructGPT, several distributed frameworks have been proposed to support the parallelization of complex InstructGPT-like RLHF training pipelines. These works include trIX [3], ColossalAI [15], DeepSpeed-Chat [33], and trl [27]. From an algorithmic aspect, these works primarily consider two RLHF model structures: AC-Share [3] and AC-NonShare [33], depending on whether the Actor and Critic model share the parameters or not. For example, in the AC-Share structure, the Actor and Critic models share parameters by adding an extra linear layer to differentiate between them. This reduces the memory and resource requirements for RLHF training, but it may potentially lead to a loss in model performance.

To parallelize the training of multiple interdependent models in the RLHF pipeline, all of these works adopt a fixed model placement strategy or its variant, referred to as the **Flattening strategy** [3], [15], [27], [33]. *The Flattening strategy straightforwardly takes four models as a whole and treats them equally.* For instance, DeepSpeed-Chat [33], one of the most popular RLHF training frameworks using the AC-NonShare structure, places all four models of RLHF pipeline on each device and applies data and model parallelism techniques like ZeRO to parallelize the training. trIX [3], another well-known

work utilizing the AC-Share structure, employs a variant of the Flattening placement strategy. It places the Reward model on a fully occupied device to leverage its computational capabilities exclusively while deploying the Actor, Critic (shared with the Actor model), and Ref model on other devices using the Flattening strategy.

However, there is an apparent issue in the trIX framework. By placing the Reward model on a single GPU device, it underutilizes both memory and computational power. If the Reward model size is too small, GPU memory is wasted, while a Reward model that is too large may lead to out-of-memory issues. Additionally, the device exclusively allocated to the Reward model will experience significant idle time within a single step. Furthermore, extra communication is required to gather the generated results using AllGather from the Actor model, and Scatter the prediction outputs back to the Actor model placed on other devices. These problems significantly degrade the overall efficiency.

Overall, unlike standard approaches for training a single model, distributed RLHF training involves managing the model placement and computation of multiple models across both training and inference runtimes. This gap creates an opportunity for further optimization to improve the training efficiency of RLHF training.

A. Limitations in Existing Distributed RLHF Training

Without loss of generality, we take the AC-Share structure as an example. Figure 1 illustrates that the Actor Generation accounts for more than 85% of the total duration in one step, while the Training stage only occupies 10% and then other forward stages using DeepSpeed-Chat. Clearly, the generation stage significantly slows down the entire RLHF training. The bottleneck comes from two main aspects: sequential execution and the fixed model placement strategy.

- **Sequential Execution.** Existing works typically follow a sequential execution order, similar to the single-machine RLHF algorithm as shown in Figure 1, where each stage or model is executed one after another. However, the generation stage is essentially more computation-intensive than other stages. The generation stage primarily involves a time-consuming autoregressive generation using the Actor model, followed by four sequential forward phases in each model. In this sequential execution order, the intermediate results generated from the time-cost generation stage in the experience replay buffer are rapidly consumed by the following stages, namely the forward and training stages. However, the training model consumes typically eight times memory as much as the inference model. Consequently, the training models are mostly idle but occupy a significant amount of memory.

- **Fixed Model Placement Strategy.** These works primarily rely on a fixed model placement strategy, namely the Flattening strategy, regardless of the size of the models used. It is easy to implement without additional intermediate data interaction and ensures that all devices keep working without idleness throughout all three stages but depends on

sequential execution ¹ However, this lack of adaptability does possess three limitations: 1) *The Flattening strategy incurs memory redundancy and additional communication costs in RLHF training.* It deploys all four models on every device, significantly reducing the available memory on each device for a single model. This necessitates an increased level of ZeRO parallelism to accommodate all models but with extra memory redundancy and communication costs, as discussed in section II-A. 2) *This strategy fails to decouple the training and inference runtime, which naturally differ from each other and require distinct optimization techniques.* In terms of parallelism, the training phase requires taking all the model states including parameters, gradients, and optimizer states into consideration, while only parameters are used in the inference phase, which requires different parallelism techniques. For example, Tensor Parallelism or PaRO [24], [31] could be used to parallelize the model inference rather than ZeRO parallelism which fits model training. 3) *Heterogeneous GPU support is difficult under this strategy.* It is due to kernel compatibility and network heterogeneity issues [6], hindering the usage of more affordable and specialized GPU series. Also, obtaining heterogeneous GPUs (e.g., a combination of A100 and V100) is comparatively easier than scheduling hundreds of homogeneous high-end GPUs in the industry [11], [30].

B. Key Challenges

To overcome these limitations, it is crucial to explore new distributed model placement strategies for efficient RLHF training, which also could save substantial costs for large-scale training prevalent in this scenario. However, to build an efficient and easy-to-use RLHF training framework, we encounter multiple challenges, including:

- **Trade-off Between Memory and Communication in Complex System.** The design of the Model Placement strategy for the RLHF system presents complexity from two perspectives. Firstly, it requires considering the intricate dependencies among each model in RLHF training. Failure to do so can result in unnecessary data interaction and device idleness aforementioned. Secondly, it needs careful trade-offs between memory and communication costs for the collective set of four models in either training or inference mode, as well as for each individual model. This necessitates considering different parallelism strategies or optimization techniques based on the scale of model size and devices.

- **High Level of Professionalism.** The development of an efficient distributed RLHF strategy is not only a demanding task in terms of design and implementation but also poses

¹Someone may argue another simple placement strategy to remove this “apparent” sequential execution order. It could exclusively place four models engaged in the Forward Stage on separate groups of devices for parallelization, given non-data dependencies among these four models during the forward stage. Nonetheless, this strategy fails to consider the interdependencies between the models across three stages. For example, the Actor model will be also utilized in the generation and training stage. During the generation stage, only devices with Actor models work, leaving other devices idle. The Flattening Strategy is more efficient than this strategy by fully utilizing all devices but heavily relies on sequential execution.

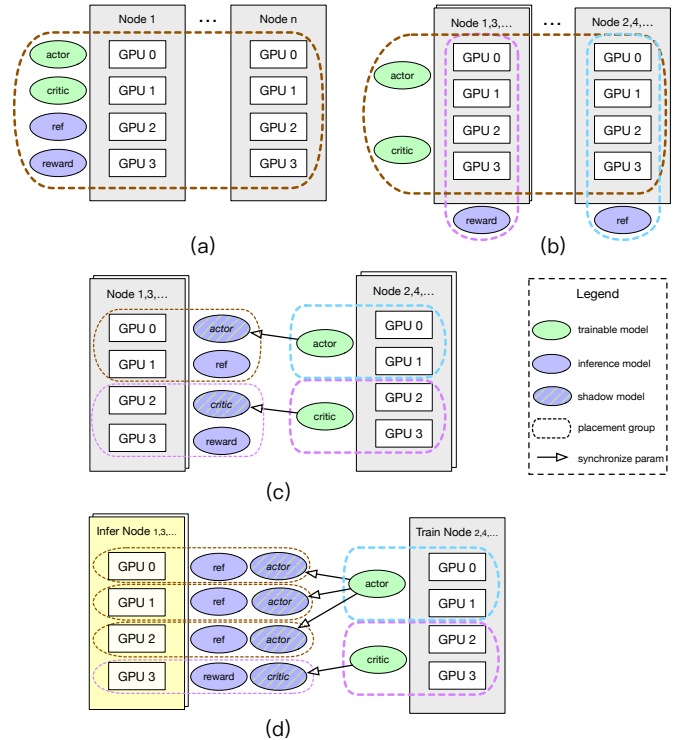


Fig. 2. The architecture of Model Placement Strategies, where (a) represents the Flattening strategy, (b) represents the Interleaving strategy, (c) demonstrates the Separation strategy used for homogeneous devices, where generation and training models are assigned to exclusive groups of devices, and (d) showcases the Separation strategy used for heterogeneous devices, where inference models are allocated to dedicated groups of devices specialized for inference.

challenges to users, particularly modeling experts who specialize in machine learning modeling but may lack knowledge in distributed computing. The usage and configuration of distributed RLHF also demand the understanding of the trade-offs involved in the distributed details to some degree. This knowledge gap can potentially hinder the efficient functioning of the distributed RLHF system in practice. Furthermore, due to the dynamic scheduling of GPUs, users are unaware of the hardware specifications during model development, also creating a gap between the model development process and the underlying hardware environment.

IV. OUR FRAMEWORK

Therefore, we introduce the Adaptive Placement and Parallelism (APP) Framework for accelerating the RLHF Training. Firstly, besides the Flattening strategy, we propose two model placement strategies aimed at enhancing the efficiency of RLHF training. These strategies are carefully designed to optimize communication efficiency and utilize memory effectively, catering to different training scenarios that involve different model scales and hardware heterogeneity. Secondly, we present the design of an APP Execution Engine abstraction, which provides modeling experts with a simplified programming API by decoupling RLHF modeling from distributed computing.

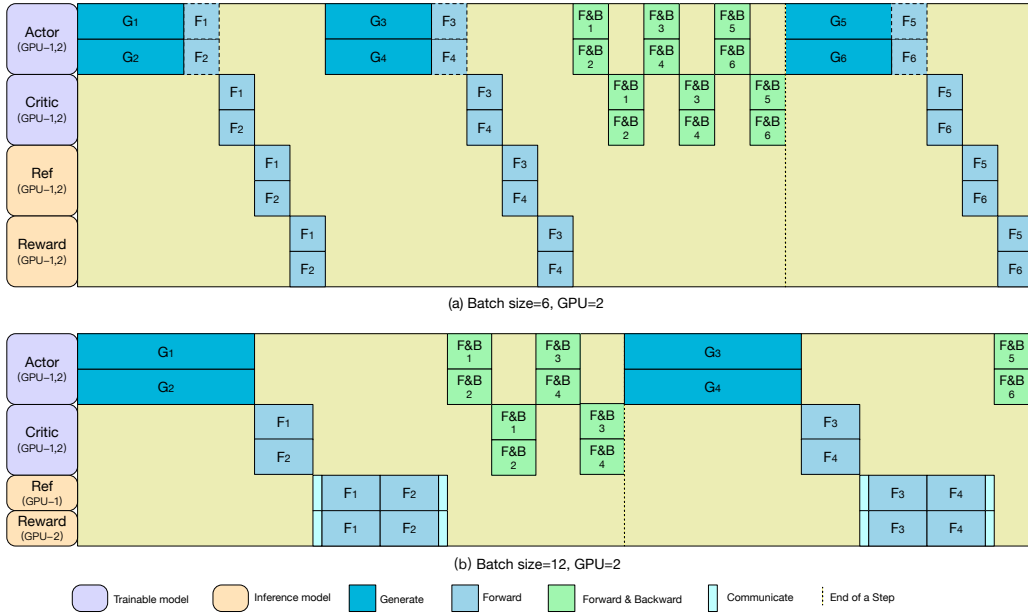


Fig. 3. The timeline of (a) Flattening strategy vs. (b) Interleaving strategy. Two homogeneous GPU devices are utilized for demonstration. Under the Flattening strategy, both the Ref model and Reward model are deployed on both devices, whereas under the Interleaving strategy, the Ref model and Reward model are allocated to separate devices. As in the figure, the efficiency improvement of the interleaving strategy is attributed to two main reasons: i) **Reduced memory redundancy**: In the Flattening strategy (a), 4 models including Actor, Critic, Ref and Reward are allocated on both GPU-1 and GPU-2, while in Interleaving strategy (b), the Ref model and Reward model are placed on GPU-1 and GPU-2 exclusively. This reduces the memory redundancy using low-level ZeRO Parallelism by reducing participating devices for the Reward model or Ref model from 2 to 1 as discussed in Section II-A. Then it allows us to increase the batch size to enhance memory utilization (as the figure illustrates, the batch size can be raised from 6 to 12). ii) **Reduced communication cost**: As the Interleaving strategy assigns the Ref model and Reward model to two separate GPU devices, it enables independent and parallel forward computation without communication between two devices in high-level ZeRO Parallelism.

A. Model Placement Strategies

1) *Interleaving Strategy*: The main idea of the Interleaving strategy is to partially parallelize the pipeline by allocating the independent models on exclusive group of GPU devices, as well as shrinking the number of computing devices required for each model. We observe that either Reward&Ref Inference (and Actor&Critic training models) could operate independently, thereby it is possible to eliminate part of the serial execution. For example, the Ref model and Reward model both take the generated responses from the Actor model as input and output the intermediate results into the experience buffer without synchronization. Also, training Actor and Critic nodes have no dependency since they do not need synchronization during the training phase. This design helps the parallelization of independent models in RLHF training. This lowers the memory redundancy and shrinks the scale of participating devices used by independent models rather than using all devices in the Flattening strategy.

We compare the distributed architecture and computation procedure between the Flattening strategy and our Interleaving strategy. We use a small number of devices as illustrative examples, while our strategy could be easily extended to large-scale computing devices. In terms of Model Placement, the Flattening strategy treats the four models as a unit and deploys them on all devices, as depicted in Figure 2(a). By contrast, our Interleaving strategy distinctly assigns the Ref model and Reward model to two distinct device groups (GPU 0-3 and

4-7)², as illustrated in Figure 2(b). It reduces the number of devices by half used by either the Ref model or the Reward model. It's important to note that responses generated from the Actor are located on GPUs where the Ref model is not placed since the Actor model is deployed on all GPU devices, as shown in the timeline in Figure 3(b). Therefore, it is necessary to perform two extra communication stages: an AllGather primitive to gather the generated results from all devices before forwarding, and then perform a Scatter primitive to distribute the results back to all devices. However, these two additional communication stages can be considered negligible by overlapping with computation. In other words, computation and communication occupy different cuda streams, allowing computation to begin upon receiving the first batch while the remaining batches can be communicated synchronously with the ongoing computation. We conclude that the Interleaving strategy shortens the time-cost generation duration from two aspects.

Firstly, in terms of memory consumption, our Interleaving strategy reduces the number of participating devices for either the Ref or Reward model, effectively minimizing memory redundancy when applying ZeRO Parallelism. This allows our method to leverage the saved memory to increase the total batch sizes, resulting in higher overall throughput. For instance, when employing the Flattening strategy as displayed in Figure

²Our interleaving strategy could further place the Actor and Critic model on exclusive devices. We only illustrate the interleaving between Reward and Ref for simplicity.

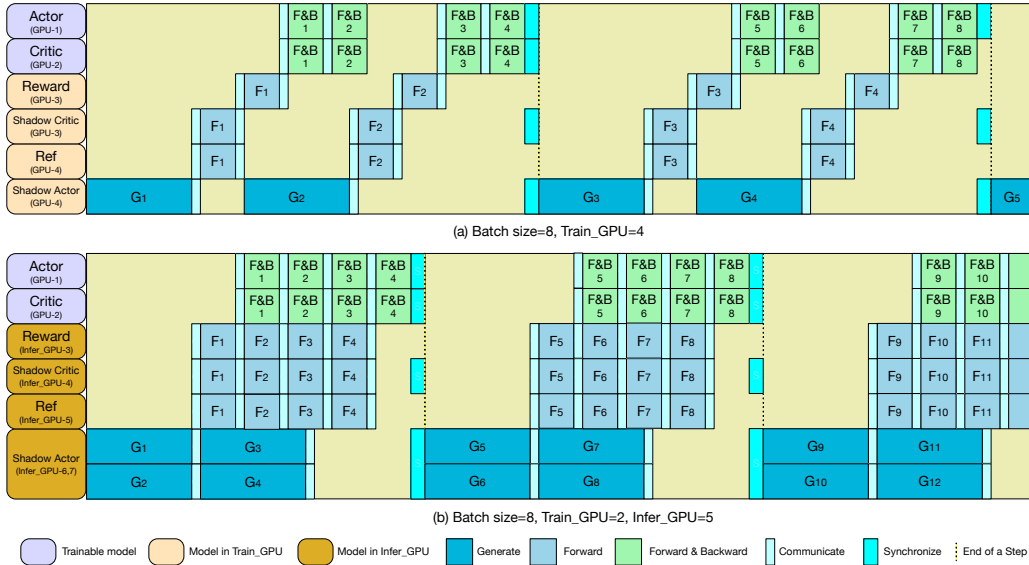


Fig. 4. The timeline of Separation strategy on homogeneous (a) and heterogeneous GPU devices (b). As illustrated in the figure, we set up shadow critic and shadow actor models and placed them on separate GPU devices (as shown in figure (a) placed on GPU-3 and GPU-4, or in figure (b) placed on the inference-dedicated GPU-4 and GPUs 6 and 7), thereby decoupling the training and inference runtime in the pipeline. Additionally, in the heterogeneous Separation strategy in (b), these two stages are designated to specialized devices for training or inference purposes. As discussed in Section IV-A2, our Separation strategy could benefit from targeted optimization for each stage. Also, this strategy does not require waiting for the entire generation process to complete before proceeding with the Forward and Forward & Backward operation with pipeline parallelism shown in (b).

3(a) under ZeRO-0, all devices hold replicas of the model states, e.g. of Reward Model, while fewer devices need to hold the replicas under our Interleaving strategy as depicted in Figure 3(b).

Secondly, from a communication efficiency perspective, having fewer participating devices leads to reduced communication overhead in both the generation and training stages. It's important to note that while increased levels of ZeRO parallelism reduce memory redundancy in model states, it comes at the cost of increased communication as discussed in Section II-B. In this case, the Interleaving strategy can further leverage high-speed intra-node bandwidth and reduce inter-node communication by colocating the Reward model or Ref model on a single machine with usually 8 GPU devices, particularly in small to medium training scenarios, e.g. 7B or 13B models.

2) *Separation Strategy*: To shorten the generation duration, our Separation strategy involves separating the training and the inference runtime of the RLHF pipeline. Specifically, we add extra shadow actor and critic models for inference only without a mixture usage of runtime. These shadow models are dedicated to inference and their parameters are synchronized with the corresponding training models periodically. This division not only allows us to run the training and generation models simultaneously but also leverages optimization techniques tailored for training or inference. It also could easily utilize the extra heterogeneous devices in clusters, since the high-end homogeneous GPU devices are scarce. Consequently, this approach significantly accelerates the generation stage and re-balance the workloads between these stages in the RLHF.

This strategy significantly speeds up the entire RLHF training, though it introduces certain memory redundancy due to additional models and communication overhead. Figure 2(c)

illustrates the placement of the training Actor and Critic models and inference models, including the Shadow Actor and Critic models, on separate devices. Optionally, we could further place the training Actor and Critic models on exclusive devices in an interleaving manner to further decrease the memory redundancy and communication costs. However, there is a need for communication for intermediate results and parameter synchronization between the training Actor/Critic models and the prediction models. Firstly, as shown in Figure 4(a), extra point-to-point communications are required before or after the Forward stage of each prediction model. Additionally, the training Actor and Critic models need to pull the intermediate results from the inference devices. These extra communication stages introduce some idle time per device, known as bubble overhead. However, these bubbles can be minimized by overlapping computation and communication stages through the use of pipeline parallelism as discussed in Section II-A. As illustrated in Figure 4(a), the bubbles are nearly hidden through micro-batching in a pipeline parallelism manner, especially with a higher number of generation times. Secondly, it is necessary to synchronize the trained model parameters between the training Actor/Critic models and shadow models after each round of PPO training. The synchronization overhead is inevitable but acceptable³.

Although this approach introduces some complexity and overhead, it provides significant benefits from three different perspectives: 1) Our Separation strategy decouples training and inference runtime of the pipeline, enabling targeted optimization

³It is critical to clarify that this process is not asynchronous training, but still synchronous training without compromising model accuracy. It thanks to the off-policy property of RLHF that the training phase involves sampling from a buffer rather than tightly following the forward stage.

techniques for each stage, as discussed in Section III-A. For example, the time-consuming Actor Generation can be accelerated by utilizing specialized parallelism strategies that are well-suited for inference workloads, such as intra-node tensor parallelism by reducing low-bandwidth inter-node communication as discussed in II. 2) The strategy also facilitates the integration of evolving inference optimizations like quantization [34], which are less compatible with model training. There will be considerable runtime swapping overheads when using a mixture of training and inference runtime. 3) The strategy allows scaling out additional heterogeneous devices tailored for training or inference workloads, especially for the time-consuming generation stage. This flexibility in either quantity or type of devices offers significant adaptability to diverse training scenarios.

B. APP Execution Engine

The APP Execution Engine is designed to provide a user-friendly interface for modeling experts to easily build their own RLHF training pipeline while hiding the messy details of distributed computing and intermediate data interaction as illustrated in Figure 5. The APP Execution Engine encapsulates each model involved in the RLHF pipeline considering both AC-Share and AC-NonShare structures. Our modular design allows for the encapsulation of each model and corresponding distributed techniques. These techniques include the model placement strategy, singular model parallelism (such as ZeRO in DeepSpeed and Tensor Parallelism in Megatron), as well as various optimization techniques in other libraries. We further the abstraction in detail:

Model Placement Abstraction. While our placement strategies offer general guidelines on how to distribute these models, there remains a gap in determining the optimal number of devices for deploying a target model, as this relies on factors like model sizes and available hardware in different training scenarios. To address this, we introduce the concept of Model Placement Ratio, which is a value ranging from 0 to 1 that represents the proportion of devices allocated for a specific model. This provides enhanced adaptability. For instance, the Flattening strategy for a Reward model has a ratio of 1, indicating that the model is deployed on all devices. On the other hand, the Interleaving strategy for the Reward model, as depicted in Figure 3, has a ratio of 0.5, signifying that the model is deployed on half of the devices. Take the Reward Model in the model placement ratio representation shown in Figure 5, e.g. [1, 1, 0.5, 0.5], as an example. The engine constructs a communication subgroup on the deployed devices of the Reward model for synchronization. It also belongs to a parent communication group that is connected with all models' subgroups for data interaction. Then our Execution Engine generates the model placement mapping, which places the model to physical devices properly according to the model placement ratio, considering the device capacity and topology, such as intra- and inter-node. This mapping involves detailed ranking assignments for each model.

```
class APPExecutionEngine:
    def __init__(self, placement_ratio, config_path):
        """placement_ratio: placement ratio for all models in RLHF. For
        four models, pass ratio of [Actor, Critic, Ref, Reward]; For six models,
        pass ratio of [Shadow Actor, Shadow Critic, Actor, Critic, Ref, Reward];
        config_path: path containing data and all model configs in RLHF"""
        self.dataloader, self.hyperparams=parse_configs(placement_ratio,
        config_path)

    def __call__(self):
        trainer = PPOTrainer(self.hyperparams)
        for batch in self.dataloader:
            experiences = trainer.generate_experience(batch)
            trainer.train_rlhf(experiences)

# e.g. a launch command for Interleaving strategy
python -m exec_engine --placement_ratio [1,1,0.5,0.5] --config_path xx
```

Fig. 5. The User interface of APP Execution Engine.

Hiding Intermediate Data Interaction. Data interaction caused by the placement strategy is also encapsulated within the Execution Engine. The Interleaving and Separation strategies introduce communication among different communication subgroups during the different stages as discussed in Section IV-A, and the APP engine handles these data interaction logics. Each training or forward operation of the models is treated as an individual Operator. The rank assigned to each model performs an AllGather operation to collect the upstream data before executing the Operator. Once the Operator is executed, the resulting data is scattered back downstream.

Overall, this abstraction enables a general interface and backend for creating a wide range of RLHF algorithms for research or industrial applications. Users can focus on the essence of RLHF modeling without being burdened by the intricacies of the underlying details, as shown in Figure 5.

V. EXPERIMENTS

We conduct comparative experiments on both AC-NonShare and AC-Share model structures against the Flattening strategy used by DeepSpeed-Chat and trIX respectively. We evaluate the model throughput while using the maximum batch size available for each framework before Out-of-Memory (OOM) for fairness. These experiments encompass variations in model sizes, device scales, and device types, allowing us to assess the effectiveness and adaptability of our APP framework across different training scenarios.

A. Experiment Settings

LLM Backbones. We employ Llama [26] of different parameter sizes as our LLM backbone, including 7B, 13B, 33B, and 65B. For demonstration purposes, we keep consistent model size for each model involved in RLHF pipeline, but our APP framework could adapt to training scenarios where each RLHF model may have varying model sizes and other LLM models, such as Opt [35].

Hyperparameters. We have established the following parameters for our research. Both the number of PPO training epochs and batches per rollout are set to 1. The input sequence length is limited to 256. Both minimum and maximum generation lengths are 256. The batch size for each experiment is set to the maximum value before Out of Memory. For other

model convergence-related parameters, we keep consistent for fairness.

Dataset. We perform RLHF on the default dataset for DeepSpeed-Chat. At the time of writing, “Dahoas/rm-static” hosted on HuggingFace is employed for tuning LLM via RLHF. This is an open-source ChatBot or Assistant style dataset, specifically designed to create a Helpful & Harmless conversational system [1].

Baseline. We conduct a comparison between the APP framework and the current state-of-the-art methods in RLHF training: DeepSpeed-Chat [33] with Hybrid Engine for the AC-NonShare case and trIX [3] for the AC-Share case.

Evaluations. We evaluate the effectiveness of different training frameworks by comparing their sample throughput during training. Sample throughput refers to the rate at which samples are processed end-to-end, typically measured in samples per second (# *samples/sec*). Furthermore, we verify that the model convergence, measured in returns, remains unaffected by our placement strategies, as evidenced in Figure 6, when compared to the DeepSpeed-Chat implementation.

Environments. Our experiments use the following software versions: CUDA 11.7, DeepSpeed 0.11.2, trIX 0.6.0, PyTorch 1.9.2, Megatron 3.0.2 and NCCL 2.14.3. The experimental cluster utilized in our study comprises up to 16 DGX nodes, with each node equipped with 8 Ampere A100 SXM3 80GB GPUs. The GPUs within each node are interconnected using NVLink, providing a high-speed bidirectional bandwidth of up to 600GB/s. In addition, the nodes are connected via 8 InfiniBand (IB) adapters, which support NVIDIA SHARP and provide around 100GB/s inter-node bandwidth.

B. Experiments and Analysis

We compare the throughput of our APP framework against DeepSpeed-Chat and trIX respectively. Specifically, in the training of the 7B model, we utilize ZeRO-2 for training models and DDP for inference models. For the training of more large models, e.g., 13B, 33B, and 65B models, we have to employ ZeRO-3 for both stages. Furthermore, our Separation strategy incorporates tensor parallelism.

1) *Comparing with DeepSpeed-Chat: Interleaving vs Flattening Strategy.* We implement two Interleaving strategies to compare them with the Flattening strategy used in DeepSpeed-Chat. In Interleaving₁, the Ref and Reward models are placed on half of the GPU devices. In Interleaving₂, we interleave not only the Ref and Reward models but also the Actor and Critic models. Based on our experiments as illustrated in Table I, we conclude that the Interleaving₁ strategy is 12% faster than the Flattening strategy in DeepSpeed-Chat in small training scenarios, such as 7B model. Additionally, the Interleaving₂ strategy is 71% faster than DeepSpeed-Chat in larger training scenarios, specifically with 65B models when employing ZeRO-3. The speedup ratio further increases when scaling out to more devices.

i) **Interleaving₁ vs. Flattening Strategy.** During the training of 7B size models using 1×8 devices, we observe that Interleaving₁ strategy in our APP framework leads to a

TABLE I

Comparing Interleaving Strategy with Flattening Strategy in DeepSpeed-Chat. The results in the table indicate the throughput of the model, measured in samples per second (# *samples/sec*). The best results are highlighted in bold.

# of GPUs	Strategy	Model Size			
		7B	13B	33B	65B
8	DeepSpeed-Chat	16.12	7.32	0.69	OOM
	Interleave ₁	17.35	7.63	0.69	OOM
2 × 8	DeepSpeed-Chat	32.15	15.35	0.64	0.14
	Interleave ₁	34.70	15.66	0.64	0.14
	Interleave ₂	18.27	8.27	0.97	0.24
4 × 8	DeepSpeed-Chat	61.95	28.60	0.93	0.20
	Interleave ₁	69.44	28.54	0.95	0.20

throughput increase from 16.12 to 17.35 samples per second, representing a speedup of 7.63% compared with Flattening strategy in DeepSpeed-Chat. This speedup ratio further improves to 12% when scaling out from 1×8 to 4×8 devices. The reason behind this improvement is that the adoption of the interleaving strategy effectively halved the memory redundancy of the Ref and Reward models. Consequently, the freed-up GPU memory can be utilized to expand the overall batch size, as explained in Section IV-A. In this case, the Interleaving strategy achieves a maximum batch size of 36, whereas DeepSpeed-Chat’s maximum batch size is 24. However, it is important to note that Interleaving₁ does not perform well with larger model scales, such as in the 33B and 65B training scenarios. This is because these models require ZeRO-3 to reduce the memory redundancy to enable training large language models, while there is no memory redundancy of model states in this case.

ii) **Interleaving₂ vs. Flattening Strategy.** In contrast, the Interleaving₂ strategy compensates for this drawback in medium to large training scenarios. Although the Interleaving₂ strategy only allocates half of the original GPU count for the Actor model, it exhibits significant improvements when combined with the ZeRO-3 mode. As shown in Table I, the Interleaving₂ strategy is respectively 52% and 71% faster than DeepSpeed-Chat in the 33B and 65B model training scenarios when using 2×8 devices. The reason behind this improvement is that, under Interleaving₂, the Actor and Reward models are placed exclusively on a single node, thus avoiding frequent inter-node AllGather communication primitives in both the prediction and training stages under ZeRO-3. Additionally, the number of communication participants for the Actor/Critic models is reduced by half.

Separation vs Flattening Strategy. The experiments for the Separation strategy are specifically conducted in large-scale training scenarios, such as training 33B and 65B models on 4 × 8 and 16 × 8 GPU devices. This is because this strategy is not well-suited for small training scenarios with a limited number of GPUs and smaller models. The reason is that the Separation strategy involves adding shadow Actor and Critic models exclusively for the prediction stage, which results in increased memory consumption.

However, the benefits of the Separation strategy are sig-

TABLE II
Homogeneous Separation strategy vs. DeepSpeed-Chat.

# of GPUs	Strategy	Model Size	
		33B	65B
4×8	DeepSpeed-Chat Separation	0.93 4.76	0.20 1.75
16×8	DeepSpeed-Chat Separation	2.11 10.07	0.55 6.80

TABLE III
Heterogeneous Separation strategy vs. DeepSpeed-Chat. We incorporate an additional 2×4 V100 GPUs for inference models to speed up the generation stage.

# of GPUs	Strategy	Model Size
		33B
1×8 A100	DeepSpeed-Chat	0.69
1×8 A100 + 2×4 V100	Heterogeneous Separation	0.79

nificant, as demonstrated in Table II. Our Separation strategy outperforms the Flattening strategy used in DeepSpeed-Chat by factors ranging from $4 \times$ to $11 \times$. For instance, in 33B model training using 4×8 GPU devices, the throughput increases from 0.93 to 4.76 samples per second, resulting in a speedup ratio of $4 \times$. The speedup ratio further increases to $7 \times$ when the model size is increased to 65B. Additionally, the Separation strategy achieves even higher speedup when scaling out to 16×8 GPU devices, reaching a speedup ratio of $11 \times$ compared to the baseline using DeepSpeed-Chat. The contribution comes from that the Separation strategy decouples the training and inference runtime of the Actor model, which is not possible for the Flattening strategy. This decoupling allows the usage of intra-node tensor parallelism for the generation stages as discussed in section IV-A. For example, in our training of 65B model using 16×8 GPUs, 3×8 devices are exclusively allocated for the Shadow Actor model. In this case, we apply tensor parallelism within the same node while replicating it across three machines. This approach significantly reduces inter-node communications compared to frequent inter-node AllGather and Scatter communications in ZeRO-3, which are required in the 33B and 65B model training for the Flattening strategy.

Heterogeneous Separation vs DeepSpeed-Chat. We also evaluate the Heterogeneous Separation strategy in a heterogeneous GPU cluster. The cluster consists of 8 A100 GPUs and an additional 8 spare V100 GPUs with 32GB memory. These heterogeneous V100 GPUs can not be utilized under the Flattening strategy. We specifically conduct experiments using large models, such as the 33B model. Under our heterogeneous Separation strategy, the Ref and Reward models are placed on a separate node with 4 V100 GPUs respectively. We enable the intra-node tensor parallelism for both models and allocate two A100 GPUs to two Shadow Actor replicas exclusively.

This configuration aims to accelerate the generation speed and improve the overall training speed.

As shown in Table III, introducing extra V100 devices under the heterogeneous Separation strategy results in a speedup of 14.49%. This acceleration increases the throughput from 0.69 to 0.79 samples per second. Although the acceleration may not be considerable due to the computing power gap between A100 and V100, this strategy explores a novel solution that allows RLHF training to utilize extra heterogeneous resources to enhance the overall throughput. It re-balances the inference workloads among different GPU devices by simply adjusting the batch size, without requiring extensive consideration of software and hardware heterogeneity among different GPUs.

2) *Comparing with trIX*: In this subsection, we compare our APP framework against trIX, which employs a variant of the Flattening strategy, in the AC-Share scenario. We evaluate our implementation of Interleaving strategies in the APP framework in terms of throughput under various computing resources. However, before presenting the experimental results, there are three important notes to mention:

i) To align the number of models with trIX for a fair comparison, our Interleaving strategy only considers the Actor, Ref, and Reward models, excluding the Critic model in terms of placement. The reason is that the Actor and Critic models share most of the parameters in AC-Share structure. The modifications required are minimal, thanks to the modular design of our model placement abstraction.

ii) We do not include comparative experiments involving the Separation or Heterogeneous Separation strategies because they are primarily effective for models with large parameter sizes, such as the 33B and 65B models. However, trIX can only place the Reward model on a single GPU, requiring the use of offloading techniques [19] to run the 33B and 65B models. However, offloading will significantly reduce the model’s prediction speed. Hence, it can be inferred that our Separation strategy offers even greater advantages in the trIX scenario compared to experiment results in DeepSpeed-Chat.

iii) In the trIX approach, there are two ways to allocate the Reward model: standalone and coexisted. In the standalone mode, the Reward model exclusively occupies a single GPU, while in the coexisted mode, the Actor model is evenly distributed across all GPUs, and the Reward model is placed on one of them. We conduct a comprehensive comparison of these two modes to evaluate their performance.

Specifically, our Interleaving strategy can achieve a speedup ratio of up to $3.6 \times$ compared with the trIX, especially with gradient checkpointing enabled⁴ and more participating nodes.

Comparison Under Gradient Checkpointing. As shown in Table IV, our Interleaving strategy without gradient checkpointing accelerated the throughput from 6.04 to 11.17 samples per second, resulting in a speedup of 84.93% for training the 6B models. This improvement arises by avoiding the single-device bottleneck in trIX, where one device is responsible

⁴Gradient checkpointing [4] refers to whether activation value recalculations are enabled during training.

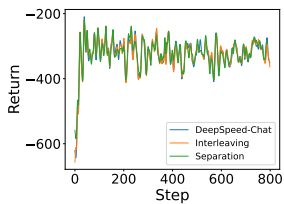


Fig. 6. Training convergence between our proposed strategies and DeepSpeed-Chat.

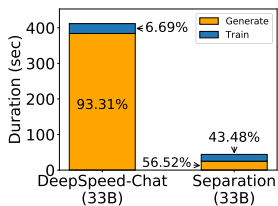


Fig. 7. Time cost between Separation strategy and DeepSpeed-Chat in generation and training.

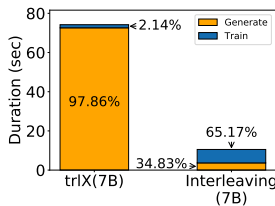


Fig. 8. Time cost between Interleaving strategy and trlX in generation and training.

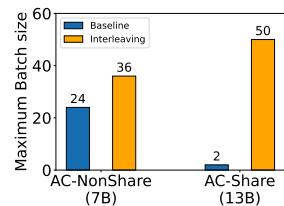


Fig. 9. Comparison of maximum available batch size in AC-NonShare and AC-Share scenarios.

TABLE IV

Comparing our Interleaving strategy with trlX on 1 machine with 8 GPU devices. Two kinds of trlX implementation are employed.

Gradient Checkpointing	Strategy	Model Size	
		7B	13B
OFF	trlX (standalone RM)	6.04	2.84
	trlX (coexisted RM)	6.20	2.20
	Interleaving	11.17	2.96
ON	trlX (standalone RM)	5.92	2.87
	trlX (coexisted RM)	6.21	2.22
	Interleaving	27.27	11.76

TABLE V

Comparing our Interleaving strategy with trlX on varying numbers of machines, each with 8 GPU devices.

# of GPUs	Strategy	Model Size	
		7B	13B
1 × 8	trlX (coexisted RM)	6.21	2.22
	Interleaving	27.27	11.76
2 × 8	trlX (coexisted RM)	7.76	3.23
	Interleaving	54.71	24.63
4 × 8	trlX (coexisted RM)	8.87	4.24
	Interleaving	109.18	46.16

for aggregating data from other devices, incurring significant communication costs and leaving other devices idle, as discussed in Section III-A. Moreover, the remaining memory that is not utilized by the Reward model is wasted, limiting the overall batch size. Also, this design leads to a longer generation duration, leaving other devices idle and resulting in underutilized resources, regardless of whether trlX is in standalone or coexisted mode. It is noteworthy that trlX narrows the performance gap when the Reward model can fully utilize the single device in 13B model training. Additionally, when gradient checkpointing is enabled, the performance gap increases significantly, resulting in a speedup ratio of 360.64%. This is because gradient checkpointing can reduce memory consumption and in turn, increase the overall training batch size. However, the single-device bottleneck in trlX disables this benefit, hindering the potential performance improvement from gradient checkpointing.

Comparison When Scaling Out. Our Interleaving strategy demonstrates significant improvements in training speed compared to trlX, which achieves acceleration ranging from 3.4× to 11×, when scaling out. As shown in Table V, our Interleaving

strategy increases the throughput from 6.21 to 27.27 samples per second, resulting in a speedup ratio of 3.4× compared to trlX for the 7B model training on 1×8 GPUs. This speedup ratio further increases to 6.1× and 11× when scaling out to 2×8 and 4×8 GPU devices respectively. The training with the 13B models exhibits a similar pattern. It is analyzed that the single-GPU bottleneck in the trlX approach significantly limited the throughput. Furthermore, the interleaving of the Reward model and Ref model in our Interleaving strategy reduces memory redundancy as discussed in Section IV-A, resulting in considerable acceleration.

3) *Detailed Analysis:* To gain a deeper understanding of the performance enhancements, we conduct further analysis of the time cost for the training and generation stages as well as the maximum batch size available for each strategy. This analysis confirms that our placement strategy significantly improves training efficiency by substantially reducing the time-consuming generation stage and enlarging the maximum batch size.

i) In the AC-NonShare scenario, we experiment with the Llama 33B model on 4×8 GPU devices. Under DeepSpeed-chat’s Flattening strategy, the generation stage occupies the majority of the total duration, accounting for 93.31% in one step, while the training stage only takes up 6.69% as illustrated in Figure 7. However, our Separation strategy reduces the overall duration in one step from around 400 seconds to 30 seconds by significantly reducing the time-consuming generation stage. The percentage of the generation stage is reduced from 93.31% to 56%, almost half of the total duration. This reduction is attributed to our Separation strategy, which allows for intra-node tensor parallelism and other inference-optimized techniques for the inference models. Additionally, our Interleaving strategy increases 50% of the maximum batch size available, from 24 to 36 compared with the DeepSpeed-Chat in the 7B model, as displayed in Figure 9.

ii) In the AC-Share scenario, we examine the time expenses for the Llama 7B model on 2×8 GPU devices. As depicted in Figure 8, our approach can reduce the overall duration from around 72 seconds to 10 seconds by largely decreasing the generation stage, as the percentage of generation duration drops from 97.86% to 34.83%. In the generation phase, the trlX approach suffers from the aforementioned single-device bottleneck. In contrast, our Interleaving strategy can speed up the generation stage by placing the Reward model on multiple devices and interleaving it with the Ref model. For the maximum batch size available, the Interleaving strategy

increases the batch size $25\times$ compared with trlX in the 13B model, rocketing up from 2 to 50, as illustrated in Figure 9.

VI. CONCLUSION

In this paper, we introduce a novel RLHF training framework that adaptively places multiple large language models in the RLHF pipeline according to different training scenarios in terms of model and device scales. Our two placement strategies, Interleaving and Separation, not only significantly enhance training efficiency but also offer adaptable solutions for different training scenarios. Additionally, our framework is easy to use and provides simple user interface.

REFERENCES

- [1] Yuntao Bai, Andy Jones, Kamal Ndousse, Amanda Askell, Anna Chen, Nova DasSarma, Dawn Drain, Stanislav Fort, Deep Ganguli, Tom Henighan, Nicholas Joseph, Saurav Kadavath, Jackson Kernion, Tom Conerly, Sheer El-Showk, Nelson Elhage, Zac Hatfield-Dodds, Danny Hernandez, Tristan Hume, Scott Johnston, Shauna Kravec, Liane Lovitt, Neel Nanda, Catherine Olsson, Dario Amodei, Tom Brown, Jack Clark, Sam McCandlish, Chris Olah, Ben Mann, and Jared Kaplan. Training a helpful and harmless assistant with reinforcement learning from human feedback, 2022.
- [2] Tom Brown, Benjamin Mann, Nick Ryder, Melanie Subbiah, Jared D Kaplan, Prafulla Dhariwal, Arvind Neelakantan, Pranav Shyam, Girish Sastry, Amanda Askell, et al. Language models are few-shot learners. *Advances in neural information processing systems*, 33:1877–1901, 2020.
- [3] Louis Castricato, Alex Havrilla, Shahbuland Matiana, Duy V. Phung, Aman Tiwari, Jonathan Tow, and Maksym Zhuravinsky. trlX: A scalable framework for RLHF, June 2023.
- [4] Tianqi Chen, Bing Xu, Chiyuan Zhang, and Carlos Guestrin. Training deep nets with sublinear memory cost. *arXiv preprint arXiv:1604.06174*, 2016.
- [5] Aakanksha Chowdhery, Sharan Narang, Jacob Devlin, Maarten Bosma, Gaurav Mishra, Adam Roberts, Paul Barham, Hyung Won Chung, Charles Sutton, Sebastian Gehrmann, et al. Palm: Scaling language modeling with pathways. *arXiv preprint arXiv:2204.02311*, 2022.
- [6] Yifan Ding, Nicholas Botzer, and Tim Weninger. Hetseq: Distributed gpu training on heterogeneous infrastructure. In *Proceedings of the AAAI Conference on Artificial Intelligence*, volume 35, pages 15432–15438, 2021.
- [7] Andrew Gibiansky. Bringing hpc techniques to deep learning, 2017.
- [8] Amelia Glaese, Nat McAleese, Maja Trkebac, John Aslanides, Vlad Firoiu, Timo Ewalds, Maribeth Rauh, Laura Weidinger, Martin Chadwick, Phoebe Thacker, et al. Improving alignment of dialogue agents via targeted human judgements. *arXiv preprint arXiv:2209.14375*, 2022.
- [9] Aaron Harlap, Deepak Narayanan, Amar Phanishayee, Vivek Seshadri, Nikhil Devanur, Greg Ganger, and Phil Gibbons. Pipedream: Fast and efficient pipeline parallel dnn training. *arXiv preprint arXiv:1806.03377*, 2018.
- [10] Yanping Huang, Youlong Cheng, Ankur Bapna, Orhan Firat, Dehao Chen, Mia Chen, HyoukJoong Lee, Jiquan Ngiam, Quoc V Le, Yonghui Wu, et al. Gpipe: Efficient training of giant neural networks using pipeline parallelism. *Advances in neural information processing systems*, 32, 2019.
- [11] Myeongjae Jeon, Shivaram Venkataraman, Amar Phanishayee, Junjie Qian, Wencong Xiao, and Fan Yang. Analysis of {Large-Scale}{Multi-Tenant}{GPU} clusters for {DNN} training workloads. In *2019 USENIX Annual Technical Conference (USENIX ATC 19)*, pages 947–960, 2019.
- [12] Xianyan Jia, Le Jiang, Ang Wang, Wencong Xiao, Ziji Shi, Jie Zhang, Xinyuan Li, Langshi Chen, Yong Li, Zhen Zheng, et al. Whale: Efficient giant model training over heterogeneous {GPUs}. In *2022 USENIX Annual Technical Conference (USENIX ATC 22)*, pages 673–688, 2022.
- [13] Zachary Kenton, Tom Everitt, Laura Weidinger, Iason Gabriel, Vladimir Mikulik, and Geoffrey Irving. Alignment of language agents. *arXiv preprint arXiv:2103.14659*, 2021.
- [14] Shen Li, Yanli Zhao, Rohan Varma, Omkar Salpekar, Pieter Noordhuis, Teng Li, Adam Paszke, Jeff Smith, Brian Vaughan, Pritam Damania, et al. Pytorch distributed: Experiences on accelerating data parallel training. *Proceedings of the VLDB Endowment*, 13(12).
- [15] Shenggui Li, Hongxin Liu, Zhengda Bian, Jiarui Fang, Haichen Huang, Yuliang Liu, Boxiang Wang, and Yang You. Colossal-ai: A unified deep learning system for large-scale parallel training. In *Proceedings of the 52nd International Conference on Parallel Processing*, pages 766–775, 2023.
- [16] Volodymyr Mnih, Adrià Puigdomènech Badia, Mehdi Mirza, Alex Graves, Timothy Lillicrap, Tim Harley, David Silver, and Koray Kavukcuoglu. Asynchronous methods for deep reinforcement learning. In *International Conference on Machine Learning*, pages 1928–1937. PMLR, 2016.
- [17] Volodymyr Mnih, Koray Kavukcuoglu, David Silver, Alex Graves, Ioannis Antonoglou, Daan Wierstra, and Martin Riedmiller. Playing atari with deep reinforcement learning. *arXiv preprint arXiv:1312.5602*, 2013.
- [18] Long Ouyang, Jeffrey Wu, Xu Jiang, Diogo Almeida, Carroll Wainwright, Pamela Mishkin, Chong Zhang, Sandhini Agarwal, Katarina Slama, Alex Ray, et al. Training language models to follow instructions with human feedback. *Advances in Neural Information Processing Systems*, 35:27730–27744, 2022.
- [19] Adam Paszke, Sam Gross, Francisco Massa, Adam Lerer, James Bradbury, Gregory Chanan, Trevor Killeen, Zeming Lin, et al. Pytorch: An imperative style, high-performance deep learning library. *Advances in neural information processing systems*, 32, 2019.
- [20] Samyam Rajbhandari, Jeff Rasley, Olatunji Ruwase, and Yuxiong He. Zero: Memory optimizations toward training trillion parameter models. In *SC20: International Conference for High Performance Computing, Networking, Storage and Analysis*, pages 1–16. IEEE, 2020.
- [21] John Schulman, Filip Wolski, Prafulla Dhariwal, Alec Radford, and Oleg Klimov. Proximal policy optimization algorithms. *arXiv preprint arXiv:1707.06347*, 2017.
- [22] Alexander Sergeev and Mike Del Balso. Horovod: fast and easy distributed deep learning in tensorflow. *arXiv preprint arXiv:1802.05799*, 2018.
- [23] Noam Shazeer, Youlong Cheng, Niki Parmar, Dustin Tran, Ashish Vaswani, Penporn Koanantakool, Peter Hawkins, HyoukJoong Lee, Mingsheng Hong, Cliff Young, et al. Mesh-tensorflow: Deep learning for supercomputers. *Advances in neural information processing systems*, 31, 2018.
- [24] Mohammad Shoeybi, Mostofa Patwary, Raul Puri, Patrick LeGresley, Jared Casper, and Bryan Catanzaro. Megatron-lm: Training multi-billion parameter language models using model parallelism. *arXiv preprint arXiv:1909.08053*, 2019.
- [25] Nisan Stiennon, Long Ouyang, Jeffrey Wu, Daniel Ziegler, Ryan Lowe, Chelsea Voss, Alec Radford, Dario Amodei, and Paul F Christiano. Learning to summarize with human feedback. *Advances in Neural Information Processing Systems*, 33:3008–3021, 2020.
- [26] Hugo Touvron, Thibaut Lavril, Gautier Izacard, Xavier Martinet, Marie-Anne Lachaux, Timothée Lacroix, Baptiste Rozière, Naman Goyal, Eric Hambro, Faisal Azhar, Aurelien Rodriguez, Armand Joulin, Edouard Grave, and Guillaume Lample. Llama: Open and efficient foundation language models, 2023.
- [27] Leandro von Werra, Younes Belkada, Lewis Tunstall, Edward Beeching, Tristan Thrush, Nathan Lambert, and Shengyi Huang. Trl: Transformer reinforcement learning. <https://github.com/huggingface/trl>, 2020.
- [28] Guanhua Wang, Heyang Qin, Sam Ade Jacobs, Connor Holmes, Samyam Rajbhandari, Olatunji Ruwase, Feng Yan, Lei Yang, and Yuxiong He. Zero++: Extremely efficient collective communication for giant model training, 2023.
- [29] Jason Wei, Maarten Bosma, Vincent Zhao, Kelvin Guu, Adams Wei Yu, Brian Lester, Nan Du, Andrew M Dai, and Quoc V Le. Finetuned language models are zero-shot learners. In *International Conference on Learning Representations*, 2021.
- [30] Qizhen Weng, Wencong Xiao, Yinghao Yu, Wei Wang, Cheng Wang, Jian He, Yong Li, Liping Zhang, Wei Lin, and Yu Ding. {MLaaS} in the wild: Workload analysis and scheduling in {Large-Scale} heterogeneous {GPU} clusters. In *19th USENIX Symposium on Networked Systems Design and Implementation (NSDI 22)*, pages 945–960, 2022.
- [31] Chan Wu, Hanxiao Zhang, Lin Ju, Jinjing Huang, Youshao Xiao, Zhaoxin Huan, Siyuan Li, Fanzhuang Meng, Lei Liang, Xiaolu Zhang, et al. Rethinking memory and communication cost for efficient large language model training. *arXiv preprint arXiv:2310.06003*, 2023.
- [32] Youshao Xiao, Shangchun Zhao, Zhenglei Zhou, Zhaoxin Huan, Lin Ju, Xiaolu Zhang, Lin Wang, and Jun Zhou. G-meta: Distributed meta learning in gpu clusters for large-scale recommender systems. In *Proceedings of the 32nd ACM International Conference on Information and Knowledge Management*, pages 4365–4369, 2023.

- [33] Zhewei Yao, Reza Yazdani Aminabadi, Olatunji Ruwase, Samyam Rajbhandari, Xiaoxia Wu, Ammar Ahmad Awan, Jeff Rasley, Minjia Zhang, Conglong Li, Connor Holmes, et al. Deepspeed-chat: Easy, fast and affordable rlhf training of chatgpt-like models at all scales. *arXiv preprint arXiv:2308.01320*, 2023.
- [34] Zhewei Yao, Reza Yazdani Aminabadi, Minjia Zhang, Xiaoxia Wu, Conglong Li, and Yuxiong He. Zeroquant: Efficient and affordable post-training quantization for large-scale transformers. *Advances in Neural Information Processing Systems*, 35:27168–27183, 2022.
- [35] Susan Zhang, Stephen Roller, Naman Goyal, Mikel Artetxe, Moya Chen, Shuohui Chen, Christopher Dewan, Mona Diab, Xian Li, Xi Victoria Lin, et al. Opt: Open pre-trained transformer language models. *arXiv preprint arXiv:2205.01068*, 2022.
- [36] Zhen Zhang, Shuai Zheng, Yida Wang, Justin Chiu, George Karypis, Trishul Chilimbi, Mu Li, and Xin Jin. Mics: Near-linear scaling for training gigantic model on public cloud. *Proc. VLDB Endow.*, 16(1):37–50, sep 2022.